Plant Biotechnology 34, 17–28 (2017)
DOI: 10.5511/plantbiotechnology.16.1231a

Original Paper

Biosynthesis of volatile terpenes that accumulate in the secretory cavities of young leaves of Japanese pepper (*Zanthoxylum piperitum*): Isolation and functional characterization of monoterpene and sesquiterpene synthase genes

Yoshiyuki Fujita[1], Takao Koeduka[1,*], Mitsuhiro Aida[2], Hideyuki Suzuki[3], Yoko Iijima[4,**], Kenji Matsui[1]

[1] Department of Biological Chemistry, Faculty of Agriculture and Division of Agricultural Sciences, Graduate School of Sciences and Technology for Innovation, Yamaguchi University, Yamaguchi 753-8515, Japan; [2] Graduate School of Biological Sciences, Nara Institute of Science and Technology, Nara 630-0192, Japan; [3] Department of Research and Development, Kazusa DNA Research Institute, Chiba 292-0818, Japan; [4] Department of Nutrition and Life Science, Kanagawa Institute of Technology, Kanagawa 243-0292, Japan
* E-mail: takaori@yamaguchi-u.ac.jp Tel: +81-83-933-5849 Fax: +81-83-933-5820
** E-mail: iijima@bio.kanagawa-it.ac.jp Tel: +81-46-206-0209 Fax: +81-46-291-3345

Received November 26, 2016; accepted December 31, 2016 (Edited by N.Sasaki)

Abstract Volatile terpenes are ones of the characteristic aromas of Japanese pepper (*Zanthoxylum piperitum*). It has been hypothesized that the specialized epithelial cells surrounding the secretory cavities of Japanese pepper fruits and leaves are responsible for the synthesis of monoterpenes and sesquiterpenes, which are generally produced by terpene synthases (TPSs); however, direct evidence for the formation of terpenes in Japanese pepper remains elusive. Here we report that monoterpenes and sesquiterpenes accumulate inside the secretory cavities of Japanese pepper leaves, but not in other parts of leaf tissues that do not include secretory cavities. We have obtained cDNAs for ZpTPS1 and ZpTPS2, which are responsible for biosynthesis of the sesquiterpenes β-caryophyllene and germacrene D, respectively, in Japanese pepper. In addition, we also identified a cDNA for the monoterpene synthase ZpTPS3. Expression of *ZpTPS3* in *Escherichia coli* in addition to *Agrobacterium*-mediated transient *ZpTPS3* expression in *Nicotiana benthamiana* demonstrated the catalytic activity of ZpTPS3 to form β-phellandrene as the major product. In situ hybridization in Japanese pepper leaf tissue revealed that *ZpTPS3* transcript specifically accumulated in the epithelial cells surrounding secretory cavities. Expression of *ZpTPS3* in epithelial cells was only detectable during early stages of cavity development, whereas the formation of volatile terpenes occurred at a constant rate throughout the expansion of secretory cavities. Our studies have improved the understanding of the currently uncharacterized processes controlling volatile terpene biosynthesis in Japanese pepper leaves.

Key words: *Agrobacterium*-mediated transient expression, epithelial cells, Japanese pepper, secretory cavity, terpene biosynthesis.

Introduction

Members of the Citrus family (Rutaceae) are some of the most popular fruit tree crop species worldwide, and commonly contain high amounts of monoterpenes and sesquiterpenes as volatile compounds in their leaves and fruit skins. These volatiles have important uses in the flavor, aromatherapy, cleaning product, and agrochemical industries because of their characteristic pleasant aromas and antimicrobial properties. For example, Japanese pepper (Rutaceae, *Zanthoxylum piperitum*) is native to East Asia and prevalent in Japan. As a result of its lemon-like aroma and pungent taste, it is commonly used in Japanese dishes as a spice and for seasoning to mask unpleasant odors that arises from fish and meat ingredients. Previous studies have shown that, after being bruised or crushed, fresh young leaves of Japanese pepper release a diverse array of terpenes, in addition to C6 volatile compounds; however, intact leaves possess almost no aroma (Jiang and Kubota 2001). Therefore, terpenes are expected to be stored in Japanese pepper leaves in the specialized structures such as trichomes and oil secretory cavities (Liang et al. 2006; Uji et al. 2015; Voo et al. 2012; Zhou et al. 2014).

This article can be found at http://www.jspcmb.jp/
Published online March 4, 2017

Many plants develop specialized organs in their leaves and stems for accumulation of volatile terpenes. On the leaf surface of herbs such as basil and peppermint, volatile terpenes are stored in a hairy organ known as a glandular trichome (Copetta et al. 2006; Voirin and Bayet 1996). Resin ducts are found in all members of the Pinaceae family and function as reservoirs of chemicals, including terpenoids, used to repel small organisms (Franceschi et al. 2005). Recent structural and chemical analyses have suggested that a diverse array of volatile terpenes, alongside bisbibenzyls, is present in oil body cells in the thallus of liverworts (Tanaka et al. 2016). Within the Rutaceae family, the most common form of such specialized structures are the secretory cavities, which are known to produce terpenes, phenolics and other plant metabolites (Uji et al. 2015; Voo et al. 2012). The secretory cavities are embedded in the sub-epidermal tissue and accumulate essential oils. In grapefruits, secretory cavities in the fruit skin are formed during early stages of fruit development, whereas the expansion of secretory cavities and essential oil accumulation occur at later stages of fruit expansion (Voo et al. 2012). In contrast, details of the biosynthetic machinery for essential oil production during secretory cavity formation in Japanese pepper remain elusive.

Although chemical analyses of volatile compounds are performed in many citrus plants, knowledge on *terpene synthase* (*TPS*) genes responsible for terpene formation in their secretory cavities is limited to rough lemon (Uji et al. 2015; Yamasaki and Akimitsu 2007). For plants native to Asia, little is known regarding the biosynthetic genes associated with terpene formation in Japanese pepper, despite a survey of specialized metabolite analysis in the genus *Zanthoxylum* (Jiang and Kubota 2001; Jiang and Kubota 2004; Sekiwa-Iijima et al. 2002). Here, we investigated terpene formation in different developmental stages of Japanese pepper leaves, and performed a detailed morphological analysis. We also identified and characterized the two sesquiterpene synthase genes, *ZpTPS1* and *ZpTPS2*, which correspond to β-caryophyllene synthase and germacrene D synthase, respectively, and one monoterpene synthase gene, *ZpTPS3*, which corresponds to β-phellandrene synthase. Characterization of enzyme activity was carried out via heterologous protein production in *Escherichia coli* and *Nicotiana benthamiana*. Furthermore, we examined the in situ localization of *ZpTPS3* transcript in Japanese pepper leaf tissues that contained secretory cavities. Our results support the notion that *ZpTPS3* encodes a monoterpene synthase mainly responsible for formation of β-phellandrene, and suggest that volatile terpenes are formed in the epithelial cells surrounding the secretory cavities of Japanese pepper leaves.

Materials and methods

Plant materials

Japanese pepper (var. Budo-sansho) was harvested at Kanja Sansyou-en (www.sansyou-en.com), Wakayama prefecture, Japan, for volatile compound analysis and RNA isolation. Plants grown in pots under a natural light environment and seasonal conditions at the Yoshida campus (E131°47′, N34°15′) of Yamaguchi University, Japan, were used for morphological analysis of leaves at different developmental stages and for in situ hybridization. Japanese pepper has an imparipinnate leaf shape, and we defined two leaflet developmental stages according to their lengths; leaflets with 0.5–5.0 mm in length were categorized as an immature developmental stage and those 0.5–2.5 cm in length were categorized as a mature developmental stage. *N. benthamiana* seeds were sown in soil in pots and cultivated in a growth room under a 14/10 h photoperiod at 25°C. Three- to four-week-old plants were used for experiments of transient expression of terpene synthase genes.

RNA-Sequencing and phylogenetic analysis

RNA-sequencing was performed as previously described by Araki et al. (2016), with minor modifications. In short, total RNA was extracted from fruit skin of Japanese pepper using a combination of the CTAB method and an RNeasy Plant Mini Kit (Qiagen Japan, Tokyo, Japan). RNA quality was evaluated using a BioAnalyzer 2100 (Agilent Technologies, Santa Clara, CA, USA). A 10-μg aliquot of total RNA was used to construct a cDNA library using an Illumina TruSeq Prep Kit v2 according to the manufacturer protocol (Illumina, San Diego, CA, USA). The resulting cDNA library was sequenced using GAIIx (Illumina) with 100 bp paired-end (PE) reads in high output mode. Total reads were assembled using CLC Genomics Workbench version 5.5.2 (CLC Bio) with the following parameters: minimum contig length: 200; perform without scaffolding to obtain assembled contigs adaptor sequences and remove low quality reads. For each sample, the reads were aligned to obtain reliable Reads Per Kilobase of exon per Million mapped reads (RPKM) values using CLC Genomics Workbench version 5.5.2 (CLC Bio).

To identify putative *Z. piperitum TPS* genes, we performed a tBLASTn search against the *Z. piperitum* Expressed Sequence Tags (EST) database using the protein sequence of *Vitis vinifera* β-caryophyllene synthase (VvCARS; GenBank accession number ADR74221; Martin et al. 2010) as the protein query, which returned five contigs. To remove those contigs that had an insignificant match to *TPS* genes, we chose only full-length genes with more than 45% homologous identity to VvCARS, which resulted in the identification of two contigs that encoded open reading frames of sesquiterpene synthases, named as *ZpTPS1* (accession number LC198039) and *ZpTPS2* (accession number LC198040). By the same approach, we identified four contigs via tBLASTn search using the protein sequence of *Citrus limon* limonene synthase (ClLIMS; GenBank accession number

AAM53944; Lücker et al. 2002) as the protein query, which were reduced to a single contig that encoded an open reading frame of monoterpene synthase, named as *ZpTPS3* (accession number LC198041).

For phylogenetic analysis, ZpTPSs were included in multiple protein sequence alignments that were performed using MAFFT v7. 220 (Katoh and Standley 2013). Gblocks 0.91b (Talavera and Castresana 2007) was utilized to remove any poorly conserved regions. MEGA6 (Tamura et al. 2013) was used to build the Maximum Likelihood tree with 1000 bootstrap repetitions. The TPS GenBank accession numbers of TPSs used for the analysis are provided in Supplementary Table S1.

Isolation of full-length cDNA of ZpTPSs

Full-length cDNA fragments of *ZpTPS1* and *ZpTPS2* were amplified from 1st-strand cDNA prepared from Japanese pepper fruit skin by reverse transcription-PCR using the gene-specific oligonucleotide primers ZpTPS1 forward primer (5′-AGT CGA CAT GGA TCT AAA GAG TAC TCT ACAA-3′; underlined bases indicate the *Sal*I-site), ZpTPS1 reverse primer (5′-ACT CGA GTT ATT TCG GAA TAG GAA GAA CAA G-3′; underlined bases indicate the *Xho*I-site), ZpTPS2 forward primer (5′-AGT CGA CAT GTC TTG TAA CGT TTC AGC AGC-3′; underlined bases indicate the *Sal*I-site), and ZpTPS2 reverse primer (5′-ACT CGA GTC ATA ACG GCA CAG GAT TAA TAA G-3′; underlined bases indicate the *Xho*I-site). The hot-start conditions were: 94°C for 2 min; 35 cycles of 98°C for 10 s, 59°C for 30 s, and 68°C for 2 min; 68°C for 5 min. Amplified PCR products were used as the template for a second-round PCR performed using the same conditions as in the first. The resulting amplified fragments with a length of 1665 bp (*ZpTPS1*) and 1674 bp (*ZpTPS2*) were ligated into the pGEM-T easy vector (Promega Co., Madison, WI, USA) and sequenced. The sequenced fragments were subcloned into the pET28b expression vector (Merck Millipore, Billerica, MA, USA) and transformed into *E. coli* Rosetta2 (DE3) pLysS cells (Merck Millipore). For transient overexpression in *N. benthamiana*, the sequenced fragments were subcloned into the pBluescript SK+ vector (Agilent Technologies), and then transferred into the pRI101-AN DNA binary expression vector (Takara Bio Inc., Shiga, Japan) to create vectors pRI101-AN-ZpTPS1 and pRI101-AN-ZpTPS2. These plasmids were then transformed into *Agrobacterium tumefaciens* GV3101 (pMP90) cells (Koncz and Schell 1986) by electroporation (Bio-Rad Micro Pulser, Agr mode; BIO-RAD, Hercules, CA, USA).

The full-length *ZpTPS3* cDNA was amplified from cDNA of Japanese pepper fruit skin by reverse transcription-PCR using the gene-specific oligonucleotide primers ZpTPS3 forward primer (5′-ATC ATA TGA TGG CAA TGT CTT CTT GCA TTA TA-3′; underlined bases indicate the *Nde*I-site) and ZpTPS3 reverse primer (5′-ACG AAT TCC TAG TAA TTA GTA CCA CGA GAT G-3′; underlined bases indicate the *Eco*RI-site). The hot-start conditions were: 94°C for 2 min; 35 cycles of 98°C for 10 s, 55°C for 30 s, 68°C for 1 min; 68°C for 5 min. For transient overexpression in *N. benthamiana*, the amplified fragment 1833 bp in length was ligated into the pGEM-T easy vector and then subcloned into the pRI101-AN DNA binary expression vector, creating the vector pRI101-AN-ZpTPS3, which was transformed into *A. tumefaciens* GV3101 (pMP90) cells. For expression in *E. coli*, ZpTPS3 coding region without 5′-end encoding chloroplast transit peptide was amplified using gene-specific oligonucleotide primers ZpTPS3 forward primer_2 (5′-CAC CAT GGC TAC TAC TGC TAG CAC CCA TCT-3′) and ZpTPS3 reverse primer_2 (5′-CTA GTA ATT AGT ACC ACG AGA TGA T-3′). The hot-start conditions were: 94°C for 2 min; 35 cycles of 98°C for 10 s, 64°C for 30 s, 68°C for 1 min; 68°C for 5 min. The amplified fragment 1710 bp in length was ligated into the pENTR/D-TOPO vector (Invitrogen, San Diego, CA, USA) and sequenced. The sequenced fragment was subcloned into the pDEST15 expression vector (Invitrogen) and transformed into *E. coli* Rosetta2 (DE3) pLysS cells.

Transient overexpression of ZpTPSs in N. benthamiana

Transient overexpression in *N. benthamiana* was performed as previously described by Bach et al. (2014) with the following modifications. *Agrobacterium* strains were cultured in YEB medium (0.5% Bacto peptone, 0.1% yeast extract, 0.5% beef extract, 0.5% sucrose, 0.11% $MgCl_2 \cdot 6H_2O$) at 28°C for 16 h. The resulting *Agrobacterium* cultures were pelleted by centrifugation (5000×*g*, 5 min) and resuspended with 1 ml of 10 mM MES buffer (pH 5.6), containing 10 mM $MgCl_2 \cdot 6H_2O$. The resuspended pellet was further diluted with sterile water to reach an OD_{600} between 0.2 and 0.4. Acetosyringone (150 μM) was added into the cell suspension before a further 2 h incubation at room temperature. *Agrobacterium* mixtures were made of a strain [GV3101 (pMP90)] carrying pRI101-AN-ZpTPS1, pRI101-AN-ZpTPS2, or pRI101-AN-ZpTPS3 combined with a strain (C58C1) carrying pBIN61-P19 and a strain [GV3101 (pMP90)] carrying pRI101-AN, which contained DNA-1-deoxy-D-xylulose-5-phosphate synthase (DXS) (Estevez et al. 2000; Mandel et al. 1996). These *Agrobacterium* mixtures were infiltrated into *N. benthamiana* leaves and infiltrated plants were incubated at 25°C for three days. Three infiltrated *N. benthamiana* leaves were harvested by cutting the petiole with a razor blade and placing the leaf tissue into a glass vial (2.7 cm diameter×12 cm height) containing 3 ml of sterile water. Vials were capped and incubated at room temperature for 16 h. Volatile compounds in vial headspace were absorbed with the solid-phase microextraction (SPME) fiber (50/30 μm DVB/Carboxen™/PDMS Stable Flex™; Sigma-Aldrich, St. Louis, MO, USA) for 30 min, before volatiles were analyzed by gas chromatography-mass spectrometry (GC-MS).

Production of recombinant ZpTPSs in E. coli and their purification

E. coli strains carrying *ZpTPS1*, *ZpTPS2*, and *ZpTPS3* in

pET28b or pDEST15 expression vectors were cultured in 2×YT medium (1.6% Bacto tryptone, 2.4% yeast extract, 0.5% NaCl), Terrific Broth medium (1.2% Bacto tryptone, 2.4% yeast extract, 0.4% glycerol, 17 mM KH_2PO_4, 72 mM K_2HPO_4), and LB medium, respectively. Production of ZpTPSs was induced by isopropyl β-D-1-thiogalactopyranoside at a concentration of 0.5 mM at 16°C for 16 h. Recombinant His-tagged ZpTPS1 and ZpTPS2 were purified from *E. coli* lysate using a His-Trap HP column (GE Healthcare UK Ltd., Buckinghamshire HP7 9NA, England) according to the manufacturer protocol. Protein purity was determined by SDS-PAGE and high-purity fractions were pooled and passed through a PD-10 column (GE Healthcare UK Ltd.) according to the manufacturer protocol to remove imidazole. Recombinant ZpTPS3 expressed as a Glutathione *S*-transferase (GST)-tagged fusion proteins was purified from *E. coli* lysate using Glutathione Sepharose 4B (GE Healthcare UK Ltd.) according to the manufacturer protocol. The purified enzymes were frozen in 20% glycerol using liquid nitrogen and stored at −80°C until further use.

Biochemical characterization of ZpTPSs

Enzymatic assays using 3.1 μg ZpTPS1, 5.7 μg ZpTPS2, or 2.3 μg ZpTPS3 were performed in 50 mM MES-KOH buffer pH 6.0 or pH 6.5 containing 20 mM $MgCl_2$, 10% glycerol, and 20 μM farnesyl diphosphate (FPP; Sigma-Aldrich) or geranyl diphosphate (GPP; Sigma-Aldrich) in a total volume of 250 μl in a 15 ml glass vial. Following 1 h incubation at 30°C, volatile compounds in the vial headspace were collected with the SPME fiber (50/30 μm DVB/Carboxen™/PDMS Stable Flex™; Sigma-Aldrich) for 30 min at 30°C, and analyzed by GC-MS.

The optimum pH was determined in buffers of 50 mM MES-KOH, 50 mM sodium phosphate, and 50 mM Tris-HCl containing 20 mM $MgCl_2$ and 10% glycerol, in the pH range from 5.0 to 9.0. Purified protein and 20 μM FPP, or GPP was used in a final volume of 250 μl. The reaction mixture was overlaid with 250 μl of hexane to trap the volatile compounds formed during the reaction. Following 1.5 h incubation at 30°C, the reaction product was extracted with 1 ml hexane. Following centrifugation, the extract was transferred into a new vial, and citronellal (0.96 μg) was added as an internal standard. The extract was concentrated under N_2 gas and analyzed by GC-MS. To determine the effect of divalent metal ions on TPS activity, Mg^{2+}, Mn^{2+}, Co^{2+}, Ni^{2+}, Zn^{2+}, or Cu^{2+} with three different ion concentrations, i.e. 0.02, 0.5, or 20 mM, were used for the enzymatic assay.

Morphometric measurements

Secretory cavities of leaflets or fruit skin from Japanese pepper were observed using a light microscope (SMZ800; Nikon, Tokyo, Japan). To observe the development of secretory cavities, immature and mature leaves were cleared by incubation in 10: 2.5: 1 chloral hydrate:water:glycerol (w/v/w) solution. They were inspected using a different interference contrast microscope (ECLIPSE Ni; Nikon) (Kunieda et al. 2008). The secretory cavity radius (r) was measured under microscope and secretory cavity volume (V) was estimated with the equation: $V=4/3\pi r^3$

In situ hybridization

In situ hybridization was performed as described by Takada et al. (2001). Immature leaves of Japanese pepper were collected and fixed in Formalin-Acetic acid-Alcohol (5 ml of 37% formalin, 2.5 ml of glacial acetic acid, 25 ml of ethanol, 17.5 ml water). The template for *ZpTPS3* sense or antisense probes 550 bp in length was prepared by PCR amplification using the gene-specific oligonucleotide primers ZpTPS3 forward primer_3 (5′-GTA TCA CAA TCA GCA TAC ACC AA-3′) and ZpTPS3 reverse primer (described above), and subcloned into the pGEM-T easy vector. Hybridization was performed at 45°C. Western Blue (Promega Co.) was used as the substrate for the signal detection.

Volatile compound analysis of Japanese pepper

For volatile compound analysis, either secretory cavities or other parts of leaf tissues were pricked with a needle (0.60 mm×32 mm; TERUMO, Tokyo, Japan) twenty times under a light microscope (SMZ800; Nikon). The pricked leaflet was immediately transferred into a glass bottle (7 cm diameter×12 cm height) and sealed. Following 10 min incubation at room temperature, the emitted volatiles in the headspace were absorbed with SPME fiber (50/30 μm DVB/Carboxen™/PDMS Stable Flex™; Sigma-Aldrich) at 25°C for 30 min, and analyzed by GC-MS. Intact leaflet samples were used as a control.

For analysis of volatile compounds from leaflets, seeds, fruit skins, or rachises, samples were ground with a mortar and pestle in liquid nitrogen, then extracted with 6 ml methyl *tert*-butyl ether (MTBE) at room temperature. After centrifugation, the extract was transferred into a new vial, and 200 μg of methyl decanoate was added as an internal standard. The extract was then analyzed with GC-MS.

GC-MS conditions

GC-MS analysis was carried out using a Shimadzu GCMS-QP2010 Plus (Kyoto, Japan). The instrument was equipped with a DB-WAX capillary column (0.25 mm i.d.×30 m×0.25 μm film thickness; Agilent Technologies). For SPME fiber analysis, samples were injected with split-mode for product analysis of ZpTPSs or with splitless-mode for volatile analysis of Japanese pepper leaflet at an initial oven temperature of 60°C (2 min hold), followed by a two-step temperature increase; first to 120°C (at a rate of 10°C min^{-1}) and then to 220°C (at a rate of 20°C min^{-1}, 12 min hold). Other parameters were injector temperature 240°C, ion source temperature 200°C; carrier gas (helium) at a flow rate of 1.39 ml min^{-1}, MS interface temperature 240°C, and split ratio 15.0. The MS was operated in the electron ionization mode with ionization energy of 70 eV. For solvent extraction analysis, samples were analyzed with the same conditions as described above, except that split ratio was 5.0.

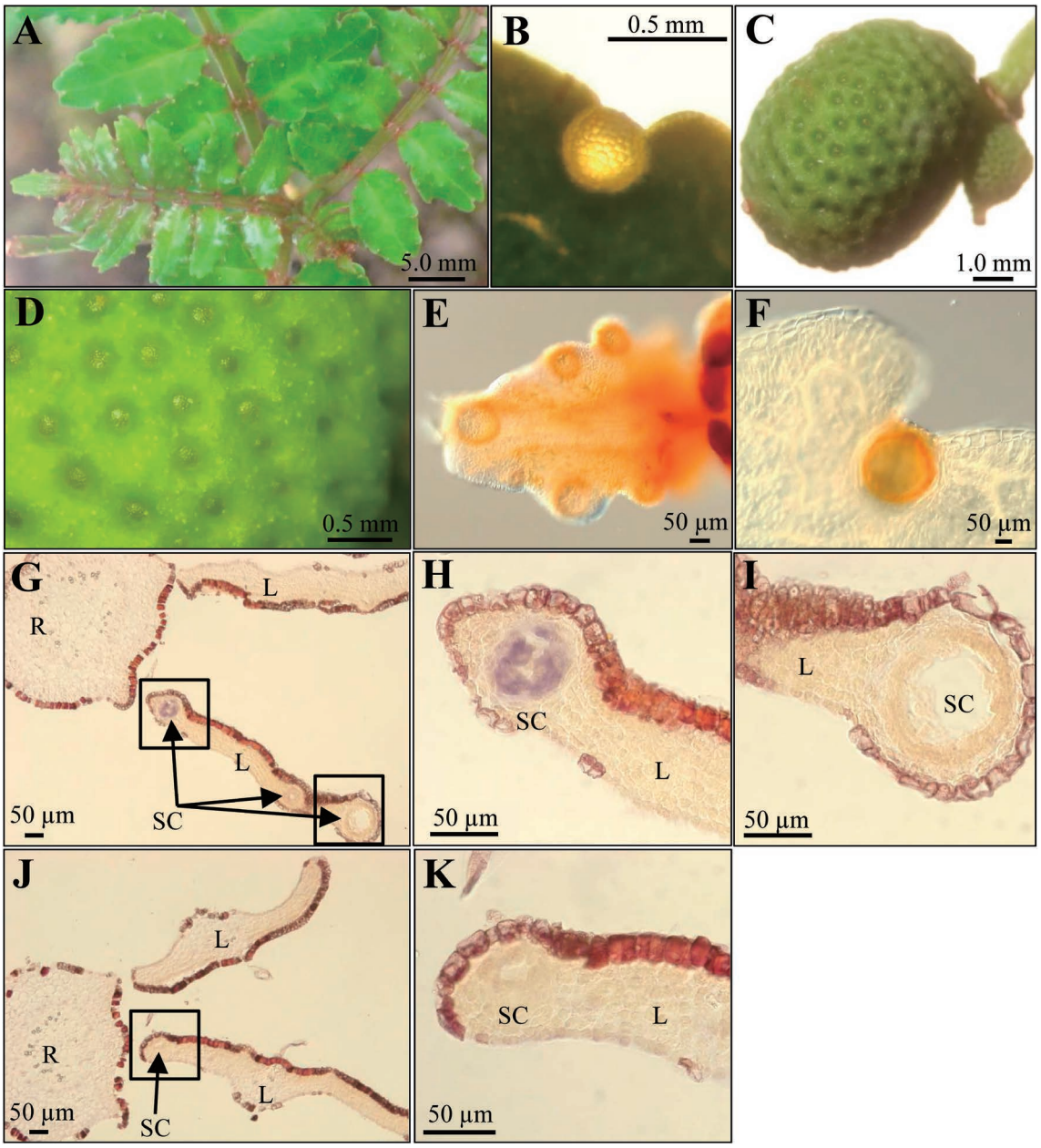

Figure 1. Photographs of the secretory cavities in fruits and leaves of Japanese pepper (A–F) and in situ localization of *ZpTPS3* mRNA in Japanese pepper leaves (G–K). (A) Shoot apex of Japanese pepper. (B) Secretory cavities of a Japanese pepper leaflet. (C) Japanese pepper fruits. (D) Magnification of fruit surface. (E) Secretory cavities in cleared leaflets at the immature developmental stage, as defined by leaflet lengths of 0.5 to 5.0 mm. (F) Secretory cavities in cleared leaflets at the mature developmental stage, as defined by leaflet lengths of 0.5 to 2.5 cm. (G–K) In situ hybridization on transverse sections of immature stage leaves. The antisense probe generated signal (purple staining) specifically in epithelial cells of immature secretory cavities (H) but not in those associated with mature cavities (I). The sense probe used as a negative control generated no signal (J–K). Brown coloring of epidermal cells is caused by an unknown reaction independent of probe hybridization. (H) and (I) are magnifications of the left and right inset squares in (G), respectively. (K) is a magnification of the inset square in (J). (G–K) L; leaflet, R; rachis, SC; secretory cavity.

Results

Morphological characterization of secretory cavities and quantitative analysis of volatile compounds in Japanese pepper leaves

Visual and microscopy analysis of Japanese pepper showed that the fruit skin, leaflets, and rachises contained many secretory cavities (Figure 1), while no secretory cavities were observed in seeds and seed skin. Secretory cavities in leaflets were present at all sinuses and formed small bulges on the surface. During immature stages of leaflet development (0.5–5.0 mm), the diameter of secretory cavities was 84.8±24.3 μm and there were 18.0±4.1 secretory cavities per leaflet (Figure 1E). In mature leaflets (0.5–2.5 cm), the diameter of secretory cavities was 122.6±17.3 μm and there were 24.5±3.1 secretory cavities per leaflet (Figure 1F).

It has been previously reported that monoterpene

hydrocarbons such as D-limonene, β-phellandrene, and β-myrcene are major components of Japanese pepper immature fruits and sesquiterpenes are present as minor components (Jiang and Kubota 2004; Sekiwa-Iijima et al. 2002). Here, we examined the levels of volatile terpenoids in the different tissues of Japanese pepper. Only low amounts of β-phellandrene, D-limonene, citronellal, β-caryophyllene, and germacrene D (68.9 μg gFW^{-1}) were detected in seeds, while 12.0 mg gFW^{-1} of volatile terpenes was extracted from exocarps (fruit skins) (Supplementary Figure S1). This result further indicates that terpenes are mostly present in the organ containing secretory cavities. We also examined the levels of volatile compounds in various leaflet tissues and found that most of volatile compounds were stored in the secretory cavities, but not in other parts of leaf tissues (Figure 2). The profiles of these volatile compounds were similar among different organs such as exocarps, leaflets, and rachises (Figures 3, Supplementary S1).

To measure the amount of volatile terpenes, we ground Japanese pepper leaflets of different developmental stages and extracted the terpenes with MTBE, which were analyzed by GC-MS. Immature leaflets contained a 2.1-fold higher amount of terpenes in fresh-weight tissue compared to that extracted from mature leaflets (Figure 4A). In contrast, the amount of terpenes in a single secretory cavity was estimated as 4.1-fold greater in mature leaflets than that in developing leaflets (Figure 4B). However, no significant difference was observed between the amounts of terpenes per volume of secretory cavities between different leaflet developmental stages (Figure 4C). These data indicate that as the Japanese pepper leaf develops, volatile terpenes gradually accumulate in the secretory cavities up to the maximum capacity of each cavity.

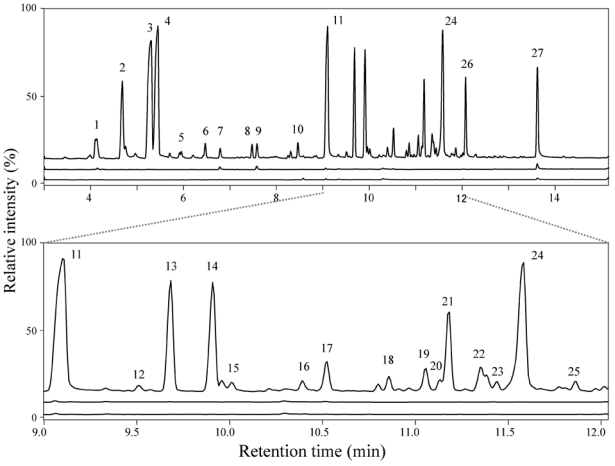

Figure 2. Headspace GC-MS analysis of the volatile compounds from Japanese pepper leaflets. Typical chromatograms obtained from the volatile compounds. From bottom to top: Total ion chromatogram obtained with volatile compounds from intact leaflets, from leaflets, whose mesophyll cells had been pricked with a needle, and from leaflets, whose secretory cavities had been pricked with a needle. The peaks are assigned to sabinene (1), β-myrcene (2), D-limonene (3), β-phellandrene (4), β-ocimene (5), 4-carene (6), (*Z*)-3-hexenyl acetate (7), isobutyl hexanoate (8), (*Z*)-3-hexenol (9), (*Z*)-methyl 4-octenoate (10), citronellal (11), α-copaene (12), β-linalool (13), linalyl acetate (14), isopulegol (15), germacrene B (16), β-caryophyllene (17), citronellol acetate (18), α-terpineol (19), α-humulene (20), α-terpineol acetate (21), citral (22), germacrene D (23), geranyl acetate (24), α-panasinsen (25), geraniol (26), and methyl cinnamate (27). Each peak was identified by comparing the compound mass spectrum to the GC-MS database.

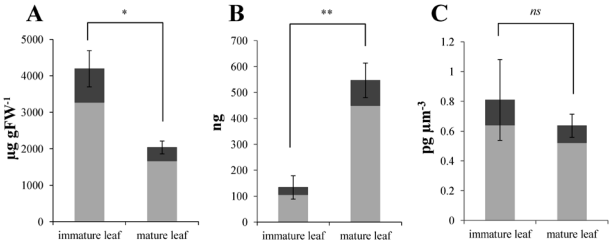

Figure 4. Terpene amount at different leaf developmental stages. (A) Terpene amount per gFW. (B) Terpene amount per secretory cavity. (C) Terpene amount per volume of secretory cavities. Monoterpenes and sesquiterpenes are indicated by gray and black, respectively. Mean values±SE are shown (n=3). Asterisks indicate significant difference (Student's t-test, *: $p<0.05$, **: $p<0.01$, *ns*: $p\geqq0.05$).

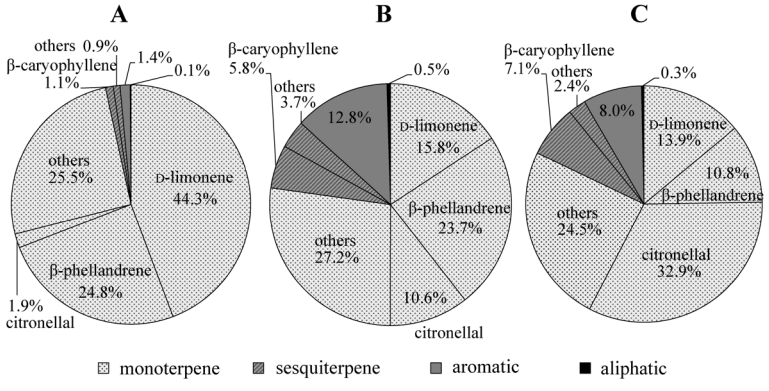

Figure 3. Volatile compound profile of different Japanese pepper tissues and organs. (A) Skin from mature fruit, (B) leaflets, and (C) rachises. Relative amounts of monoterpene, sesquiterpene, aromatic compound, and aliphatic volatiles are presented as a percentage of each class.

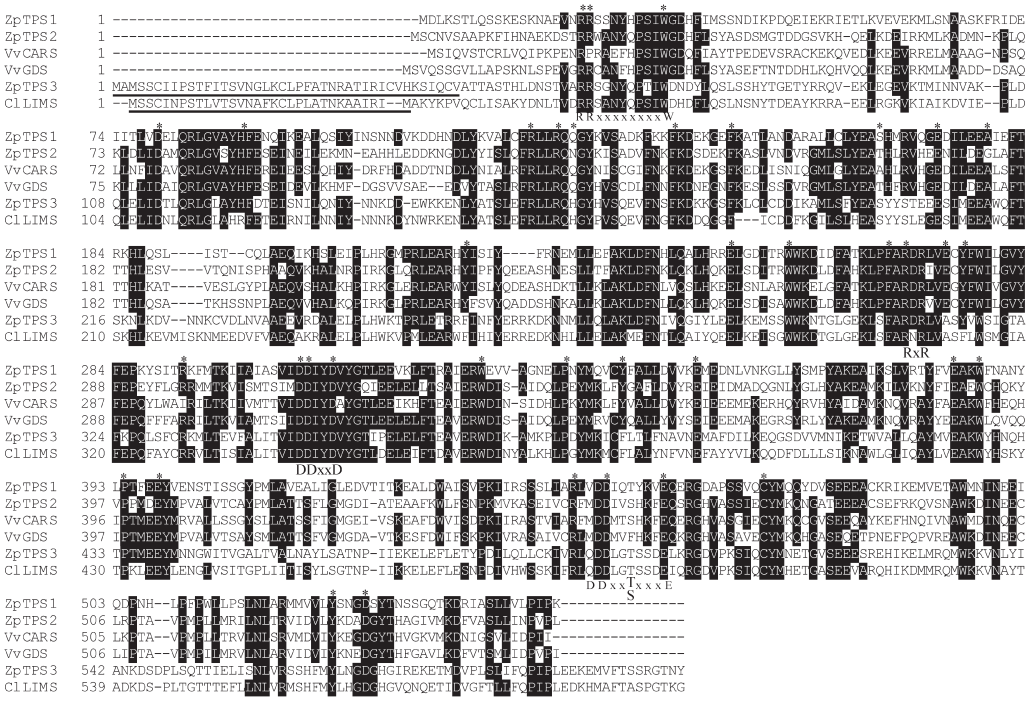

Figure 5. Amino acid sequence alignment of ZpTPSs, *β*-caryophyllene synthase (VvCARS; ADR74221) and germacrene D synthase (VvGDS; AAS66357.1) from *Vitis vinifera*, and limonene synthase from *Citrus limon* (ClLIMS; AAM53944.1). The program GENETYX-MAC Ver.12.2.0 was used for the alignment. Black highlighting indicates those residues with more than 50% conservation among all sequences. Asterisks indicate residues that are highly or absolutely conserved between all plant TPSs (Lücker et al. 2002). The putative chloroplast transit peptide is underlined. The canonical highly conserved regions are labeled with $RR(x)_8W$, RxR, DDxxD and DDxx(S, T)xxxE (Huang et al. 2013).

Cloning and sequence analysis of ZpTPSs

Using the protein sequence of *V. vinifera β*-caryophyllene synthase (Martin et al. 2010) or *C. limon* limonene synthase (Lücker et al. 2002) as a query, a BLAST analysis of the EST database of Japanese pepper fruit skin revealed two sesquiterpene synthase-like sequences, named as *ZpTPS1* and *ZpTPS2*, and one monoterpene synthase-like sequence, named as *ZpTPS3*. The deduced amino acid sequences of *ZpTPS1* and *ZpTPS2* were 50% and 73% identical to that of sesquiterpene synthases from *V. vinifera* that produce *β*-caryophyllene (VvCARS; Martin et al. 2010) and from *Citrus jambhiri* that produce *δ*-elemene (CjELES; Uji et al. 2015), respectively, whereas that for ZpTPS3 displayed highest similarity to monoterpene limonene synthase of *C. limon* (ClLIMS; Lücker et al. 2002) with 65% identity at the amino acid level. The ORFs for *ZpTPS1* and *ZpTPS2* encoded proteins 554 and 557 amino acids in length with predicted molecular masses of 64.4 and 64.7 kDa, respectively. The ORF for *ZpTPS3* encoded a protein 610 amino acids in length with a molecular mass of 70.7 kDa. ZpTPS3 contained a predicted N-terminal chloroplast transit peptide (ChloroP 1.1; www.cbs.dtu.dk/services/ChloroP) composed of 42 amino acids, which resembled other plant monoterpene synthase chloroplast transit peptides (Demissie et al. 2011; Lücker et al. 2002). In contrast, no chloroplast transit peptides were predicted in ZpTPS1 and ZpTPS2. Furthermore, each of the three ZpTPS proteins contained all conserved TPS domains including the DDxxD, DDxx(S, T)xxxE, $RR(x)_8W$, and RxR motifs (Figure 5) (Huang et al. 2013). ZpTPS1 and ZpTPS2 shared 48.4% sequence identity, while ZpTPS3 shared 40.0% and 35.3% sequence identity with ZpTPS1 and ZpTPS2, respectively.

To analyze the phylogenetic relationships of the ZpTPSs with known TPSs from other plants, a phylogenetic tree was constructed using the Maximum likelihood method (Figure 6). The TPS family in plants has been classified into seven subfamilies, namely TPSa to TPSg, as described previously (Bohlmann et al. 1998; Dudareva et al. 2003). ZpTPS1 and ZpTPS2 were categorized into the cluster of angiosperm sesquiterpene synthases (TPSa), whereas ZpTPS3 was classified into the cluster of angiosperm monoterpene synthases (TPSb).

Functional characterization of ZpTPSs

To test enzymatic activity of ZpTPSs in vitro, recombinant proteins were produced in *E. coli* cells. Recombinant proteins were purified using His-tag or GST-tag affinity chromatography (Supplementary Figure S2) and assayed with the potential substrates FPP or GPP. The optimum pH for activity of each ZpTPS ranged from 6.0 to 6.5 with MES-KOH buffer (data not shown). ZpTPS1 specifically accepted the substrate FPP and produced the sesquiterpenes *β*-caryophyllene (89.1% of total products) and *α*-humulene (10.9% of total

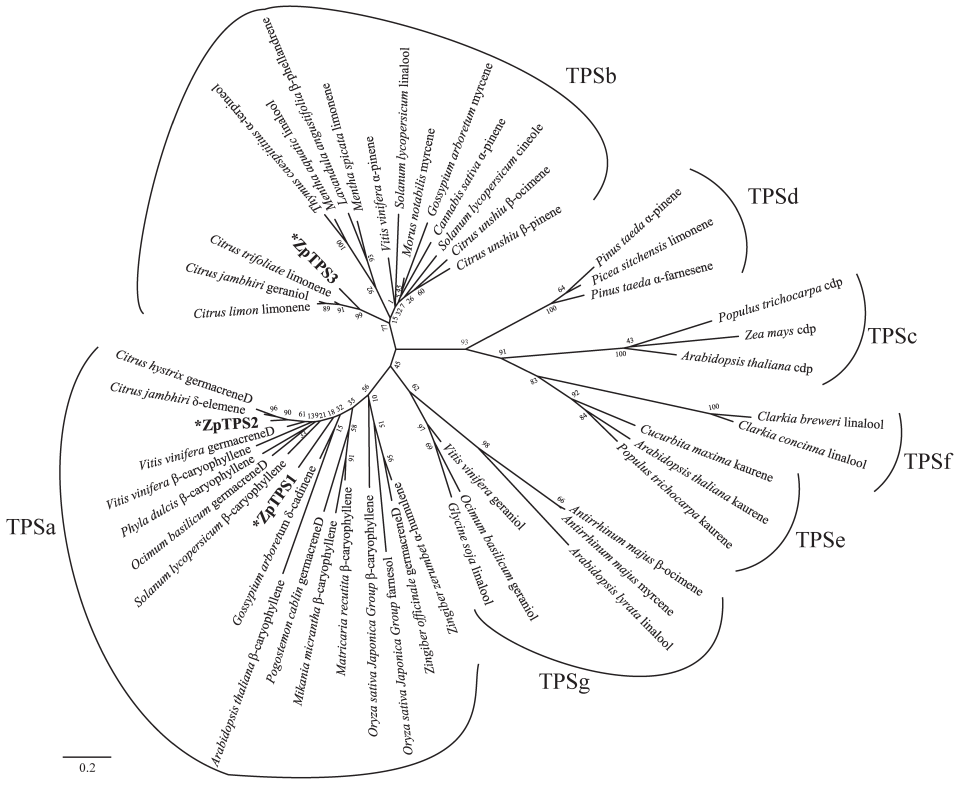

Figure 6. Phylogenetic analysis of TPS protein family. Phylogenetic analysis was performed in MEGA6 using the maximum likelihood method. Asterisks indicate the ZpTPSs identified in this study. TPSa consists of sesquiterpene synthases from angiosperms, TPSb consists of monoterpene synthases from angiosperms, TPSc consists of copalyl diphosphate synthases, TPSd consists of terpene synthases from gymnosperms, TPSe consists of kaurene synthases, TPSf consists of linalool synthases from *Clarkia*, and TPSg consists of terpene synthases that lacked the specific motif of general TPSs (Bohlmann et al. 1998; Dudareva et al. 2003). Accession numbers are provided in Supplementary Table S1.

products) (Figure 7). Reaction product identification was confirmed by comparing retention times and mass spectra with those of β-caryophyllene and α-humulene standards. ZpTPS2 also utilized FPP as a substrate and predominately produced germacrene D (peak No. 14 in Figure 7E; 43.6% of total products) alongside eighteen C15 compounds including two putative sesquiterpenes, germacrene B (12.5% of total products), and δ-cadinene (7.8% of total products) as minor products (Figure 7E). This catalytic activity by ZpTPS2 was confirmed by comparison with the products by ginger germacrene D synthase (*Zingiber officinale*; Picaud et al. 2006) (Figure 7D). On the other hand, ZpTPS3 specifically accepted GPP as a substrate and produced mainly β-phellandrene (57.9% of total products) alongside four C10 compounds including β-myrcene (18.1% of total products) and D-limonene (20.4% of total products) as co-products (Figure 8). An extract of an empty-vector *E. coli* strain was used as a negative control and did not produce detectable TPS products (data not shown), suggesting that these reaction products were enzymatically produced.

Terpene synthases have an absolute requirement for divalent metal ions as a cofactor (Rajaonarivony et al. 1992; Starks et al. 1997). Therefore, the activity of ZpTPSs has been measured in the presence of several different divalent metal ions such as Mg^{2+}, Mn^{2+}, Co^{2+}, Ni^{2+}, Zn^{2+}, and Cu^{2+} (Supplementary Figure S3). ZpTPS1 displayed the highest activity in the presence of 20 mM Mg^{2+}. The relative activity of ZpTPS1 with Co^{2+} (at 0.5 mM), Mn^{2+} (at 0.02 mM), Zn^{2+} (at 0.02 mM), and Ni^{2+} (at 0.5 mM) was 94.5%, 69.4%, 58.0%, and 13.4%, respectively. However, ZpTPS1 displayed negligible activity in the presence of Cu^{2+}. For ZpTPS2, the highest activity was observed in the presence of Mg^{2+} (at 20 mM) followed by lesser activities with Co^{2+} (55.9% relative activity at 0.5 mM), Mn^{2+} (20.1% at 0.5 mM), and Ni^{2+} (4.1% at 0.5 mM). ZpTPS2 was inactive in the presence of Zn^{2+} and Cu^{2+}. ZpTPS3 displayed highest activity in the presence of Mg^{2+} (at 20 mM) and Mn^{2+} (at 0.5 mM) followed by lesser activities with Co^{2+} (32.8% at 0.5 mM), Zn^{2+} (20.9% at 0.02 mM), and Ni^{2+} (1.4% at 0.5 mM). ZpTPS3 was inactive in the presence of Cu^{2+}.

To further confirm the biochemical function of ZpTPSs *in planta*, *ZpTPS* genes were over-expressed in *N. benthamiana* leaves using the *Agrobacterium*-mediated transient gene expression system. DXS was co-produced with ZpTPSs in *N. benthamiana* leaves. DXS catalyzes the first step of the methylerythritol phosphate pathway (Estevez et al. 2000), resulting

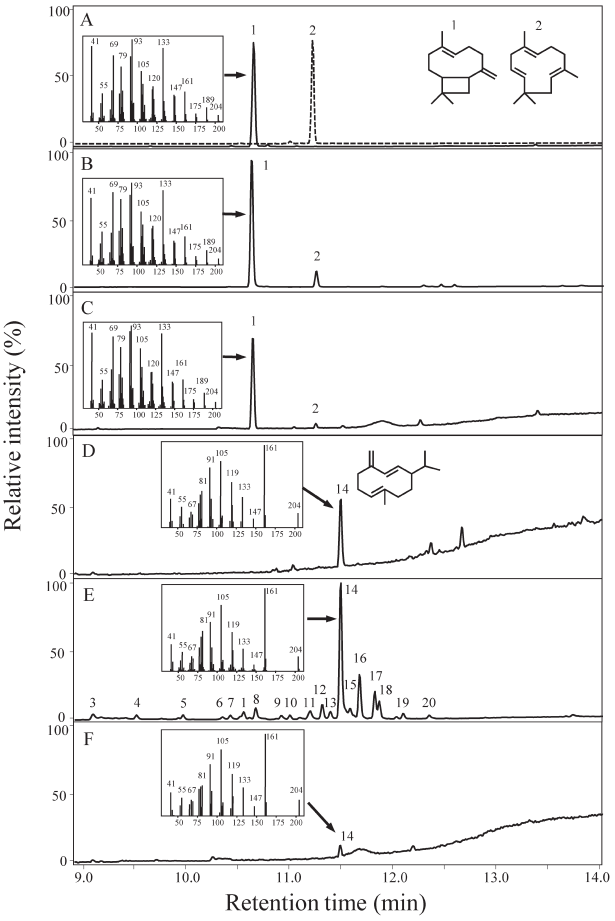

Figure 7. Identification of the products of ZpTPS1 and ZpTPS2 activity by GC-MS analysis. (A) Standards of *β*-caryophyllene (indicated by the solid black line) and *α*-humulene (indicated by the dahsed black line). (B) The products generated by recombinant ZpTPS1 with FPP substrate. (C) The products generated by transiently produced ZpTPS1 with endogenous substrates in *N. benthamiana* leaves. (D) The products generated by germacrene D synthase of ginger (*Z. officinale*, Picaud et al. 2006), included as a positive control. (E) The products generated by recombinant ZpTPS2 with FPP substrate. (F) The products generated by transiently produced ZpTPS2 with endogenous substrates in *N. benthamiana* leaves. (A-F) Labeled peaks are sesquiterpenes: *β*-caryophyllene (1), *α*-humulene (2), unknown (3), *α*-copaene (4), *α*-cubebene (5), isoledene (6), *β*-elemene (7), alloaromadendrene (8), *β*-cadinene (9), unknown (10-12), ledene (13), germacrene D (14), *α*-muurolene (15), germacrene B (16), *δ*-cadinene (17), *γ*-muurolene (18), unknown (19), and calamenene (20). Reaction products were identified by GC-MS according to the MS-library database.

in increased endogenous supply of GPP or FPP for TPSs in *N. benthamiana* leaves. It has been reported that over-expression of DXS in spike lavender led to increased essential oil production (Muñoz-Bertomeu et al. 2006). At three days post *Agrobacterium* infiltration extracts of *N. benthamiana* leaves were analyzed by GC-MS. Sesquiterpenes *β*-caryophyllene (96.0% of total products) and *α*-humulene (4.0% of total products) were specifically detected in *N. benthamiana* leaves heterologously expressing *ZpTPS1* gene (Figure 7C), and germacrene D in the *N. benthamiana* leaves heterologously expressing *ZpTPS2* gene (Figure 7F). The *N. benthamiana* leaves producing ZpTPS3 predominately accumulated *β*-phellandrene (69.5% of total products) in addition to three C10 compounds including *β*-myrcene (12.2% of total products) and D-limonene (17.2% of total products) as minor co-products (Figure 8C). In contrast, those *N. benthamiana* leaves infiltrated with *Agrobacterium* carrying an empty vector, which served as the negative control, did not produce any detectable C10 or C15 compounds (data not shown).

In situ hybridization of ZpTPS3 gene transcripts in Japanese pepper leaf tissue

To clarify the regional enrichment of monoterpenes to the cavity, subcellular localization of transcripts of *ZpTPS3* was investigated by in situ hybridization on serial sections of developing Japanese pepper leaves. A labelled antisense RNA probe for *ZpTPS3* detected transcripts of the gene specifically in the epithelial cells of the immature leaflet secretory cavities (Figure 1H). The majority of signal was restricted to smaller developing cavities, and no staining was observed in large, mature secretory cavities (Figure 1I). In the negative control, where a sense probe was used, no staining was observed (Figure 1J, K).

Discussion

Localization of volatile compounds

Previous studies have reported that the leaves and fruit skin of citrus plants generally have secretory cavities, which are embedded in subepidermal tissues and accumulate essential oils (Voo et al. 2012). Similarly, Japanese pepper, a member of the genus *Zanthoxylum*, was found to contain secretory cavities in the tissues tested in this study, which included leaflets, rachises, and fruit skin (Figure 3). However, unlike known secretory cavities, those in Japanese pepper formed small bulges on the surface of leaflet tissue due to their significant expansion (Figure 1). In organs, such as seeds, that do not have any secretory cavities, only few volatile compounds were detected (Figure S1), indicating that the majority of volatile compounds are present in those organs that contain secretory cavities. Furthermore, to characterize the localization of volatile compounds in detail, we analyzed the levels of volatile compounds in different areas of leaflet tissue, suggesting that the majority of volatile compounds were detected in the secretory cavities (Figure 2). These results indicate that Japanese pepper, which belongs to the genus *Zanthoxylum*, possesses typical characteristics of secretory cavities that accumulate volatile compounds as is observed in plants to the genus *Citrus*.

It has been generally believed that specific localization of volatile compounds produced by plants contributes

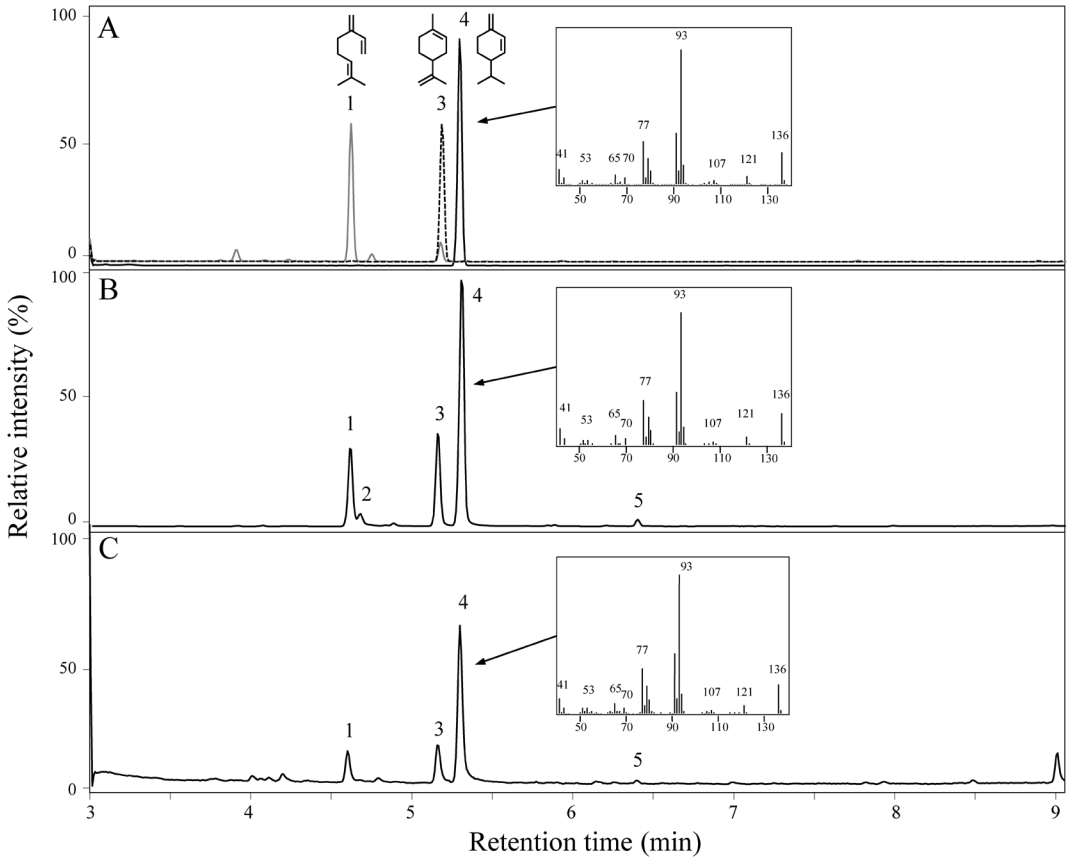

Figure 8. Identification of the products of ZpTPS3 activity by GC-MS analysis. (A) Standard of *β*-phellandrene (indicated by the solid black line), *β*-myrcene (indicated by the gray line), and D-limonene (indicated by the dashed black line). (B) Analysis of the products generated by recombinant ZpTPS3 with GPP substrate. (C) The products generated by transiently produced ZpTPS3 with endogenous substrate in *N. benthamiana* leaves. (A-C) Labeled peaks are monoterpenes: *β*-myrcene (1), *α*-phellandrene (2), D-limonene (3), *β*-phellandrene (4), and 4-carene (5). Reaction products were identified by GC-MS according to the MS-library database.

defense against herbivore and pathogen attack. When the secretory cavities were pricked, the secretory cavity contents quickly leaked out the tissues. It is most likely that volatile terpenes accumulated in the secretory cavities are involved in defense against insect damage. On the other hand, it is well known that volatile terpenes-producing Citrus plants including Japanese pepper are hosts for the larvae of a swallowtail butterflies (Honda and Hayashi 1995; Ômura et al. 2006). When the chemical composition in the osmeterial secretions from larvae of some swallowtail species of the tribe Papilionini was analyzed, volatile terpenes including D-limonene, *β*-phellandrene, and *β*-caryophyllene were detected, suggesting that ZpTPSs might contribute to ecological interaction between a swallowtail and Japanese pepper via volatile terpenes. Further experiments in detail ecological and physiological function of volatile terpenes in Japanese pepper will be required.

Development of secretory cavities and biosynthesis of volatile compounds in Japanese pepper

A quantitative analysis of volatile terpenes in Japanese pepper leaflets of different developmental stages showed that the amount of terpenes per one secretory cavity in mature leaflets was 4.1-fold greater than that in immature leaflets, while there was no significant difference in the amount of terpenes per volume of secretory cavities in leaflets of different developmental stages (Figure 4). This result suggests that the cavity size is increased depending on the accumulation of volatile terpenes during the development of Japanese pepper fruits.

In our investigation in RNA-seq data of Japanese pepper fruits, we have observed the similar RPKM values among *ZpTPS1, ZpTPS2, ZpTPS3*, and other *TPS-like genes* (Supplementary Table S2), but the contents of monoterpenes in the fruit skins is much more than that of sesquiterpenes (Figure 3). However, there is no significant difference of RPKM values between geranyl diphosphate synthase-like genes and farnesyl diphosphate synthase-like genes, which synthesize the endogenous substrates for monoterpene synthases and sesquiterpene synthases, respectively (Supplementary Table S2). Thus, the compositional ratio of monoterpenes and sesquiterpenes in Japanese pepper fruits might be regulated by the protein levels such as posttranslational

modification.

In addition to β-phellandrene, one of the major monoterpenes accumulated in Japanese pepper fruits is D-limonene. This observation suggests that, in addition to *ZpTPS3* genes, other biosynthetic enzymes to form volatile terpenes also contribute the production of D-limonene in the fruits. This hypothesis is consistent with the observations that several cDNAs with conserved domains found in TPS family have been found to be expressed in the EST database of Japanese pepper fruits (Supplementary Table S2).

Following in situ hybridization experiments in Japanese pepper leaves, we found that *ZpTPS3* transcripts were specifically located in the epithelial cells surrounding secretory cavities (Figure 1H), which indicated correlation between the site of terpenoid synthesis and its accumulation. Similar results have been reported for transcripts of *limonene, sabinene*, or *δ-elemene synthase* in rough lemon leaves (Uji et al. 2015; Yamasaki and Akimitsu 2007). In rough lemon, expression of *TPS* genes was detected both in mature and developing secretory cavities. In contrast, staining was specifically detected in Japanese pepper in developing but not mature secretory cavities. This indicates that the majority of *ZpTPS3* expression occurs in early stages of secretory cavity development before it is downregulated upon cavity maturation. Thus, our results demonstrate that, while the spatial *TPS* gene expression patterns are relatively similar between the two citrus species, there are temporal differences in gene expression, and this may be useful in further understanding of diversification of terpene biosynthesis in citrus plants.

Evolutionary relatedness of ZpTPS1, ZpTPS2, and ZpTPS3 to other TPS proteins

Although there have been many studies concerning volatile terpene profiles in citrus plants, this report presents the first characterization of three TPSs, namely β-caryophyllene synthase, germacrene D synthase, and β-phellandrene synthase, in a member of the genus *Zanthoxylum*. Our phylogenetic analyses indicate that ZpTPS1 and ZpTPS2 fall into a cluster in which proteins characterized to have sesquiterpene synthase activity, and that ZpTPS3 is closely related to a cluster that contains protein biochemically characterized to possess limonene synthase activity except *Citrus jambhiri* geraniol synthase (Figure 6). In the latter cluster, since ZpTPS3 is capable of synthesizing limonene as co-products, it is most likely that the ancestral protein in this cluster had limonene synthase activity, then function of ZpTPS3 and *Citrus jambhiri* geraniol synthase have been derived recently from their ancestral function via biochemical differentiation.

Recent studies of in vitro mutagenesis experiments in limonene synthase of spearmint (Srividya et al. 2015) suggest that the residues W324 and H579 play critical roles in the stabilization of intermediate carbocations and the high fidelity to form limonene specifically. In addition to these two residues, N345 and M458 in limonene synthase of spearmint are also major determinant of product specificity. The corresponding positions of W324 and H579 in limonene synthase of spearmint are conserved in ZpTPS3, but the amino acid residues at equivalent positions to N345 and M458 in spearmint limonene synthase are not conserved both in ZpTPS3 and in limonene synthase of *Citrus limon* and *Citrus trifoliate* (Supplementary Figure S4). This suggests that these four amino acid residues do not function as active sites to determine product specificity in ZpTPS3.

Acknowledgements

We thank Mr. Tsutomu Hosouchi and Ms Sayaka Shinpo, Kazusa DNA Research Institute for technical support in Illumina sequencing. This research was partly supported by the Japan Society for the Promotion of Sciences KAKENHI Grants 15K18690 (to T.K.) and 15H02893 (to Y.I.).

References

Araki T, Saga Y, Marugami M, Otaka J, Araya H, Saito K, Yamazaki M, Suzuki H, Kushiro T (2016) Onocerin biosynthesis requires two highly dedicated triterpene cyclases in a fern *lycopodium clavatum*. *Chem Bio Chem* 17: 288–290

Bach SS, Bassard J-É, Andersen-Ranberg J, Møldrup ME, Simonsen HT, Hamberger B (2014) High-throughput testing of terpenoid biosynthesis candidate genes using transient expression in *nicotiana benthamiana*. *Methods Mol Biol* 1153: 245–255

Bohlmann J, Meyer-Gauen G, Croteau R (1998) Plant terpenoid synthases: Molecular biology and phylogenetic analysis. *Proc Natl Acad Sci USA* 95: 4126–4133

Copetta A, Lingua G, Berta G (2006) Effects of three AM fungi on growth, distribution of glandular hairs, and essential oil production in *Ocimum basilicum* L. var. *Genovese*. *Mycorrhiza* 16: 485–494

Demissie ZA, Sarker LS, Mahmoud SS (2011) Cloning and functional characterization of β-phellandrene synthase from *Lavandula angustifolia*. *Planta* 233: 685–696

Dudareva N, Martin D, Kish CM, Kolosova N, Gorenstein N, Fäldt J, Miller B, Bohlmann J (2003) (*E*)-β-ocimene and myrcene synthase genes of floral scent biosynthesis in snapdragon: Function and expression of three terpene synthase genes of a new terpene synthase subfamily. *Plant Cell* 15: 1227–1241

Estevez JM, Cantero A, Romero C, Kawaide H, Jimenez LF, Kuzuyama T, Seto H, Kamiya Y, Leon P (2000) Analysis of the expression of *CLA1*, a gene that encodes the 1-deoxyxylulose 5-phosphate synthase of the 2-*C*-methyl-D-erythritol-4-phosphate pathway in Arabidopsis. *Plant Physiol* 124: 95–104

Franceschi VR, Krokene P, Christiansen E, Krekling T (2005) Anatomical and chemical defenses of conifer bark against bark beetles and other pests. *New Phytol* 167: 353–376

Honda K, Hayashi N (1995) Chemical nature of larval osmeterial secretions of papilionid butterflies in the genera *Parnassius, Sericinus* and *Pachliopta*. *J Chem Ecol* 21: 859–867

Huang X, Xiao Y, Köllner TG, Zhang W, Wu J, Wu J, Guo Y,

Zhang Y (2013) Identification and characterization of (*E*)-*β*-caryophyllene synthase and *α*/*β*-pinene synthase potentially involved in constitutive and herbivore-induced terpene formation in cotton. *Plant Physiol Biochem* 73: 302–308

Jiang L, Kubota K (2001) Formation by mechanical stimulus of the flavor compounds in young leaves of Japanese pepper (*Xanthoxylum piperitum* DC.). *J Agric Food Chem* 49: 1353–1357

Jiang L, Kubota K (2004) Differences in the volatile components and their odor characteristics of green and ripe fruits and dried pericarp of Japanese pepper (*Xanthoxylum piperitum* DC.). *J Agric Food Chem* 52: 4197–4203

Katoh K, Standley DM (2013) MAFFT multiple sequence alignment software version 7: Improvements in performance and usability. *Mol Biol Evol* 30: 772–780

Koncz C, Schell J (1986) The promoter of T_L-DNA gene 5 controls the tissue-specific expression of chimaeric genes carried by a novel type of *Agrobacterium* binary vector. *Mol Gen Genet* 204: 383–396

Kunieda T, Mitsuda N, Ohme-Takagi M, Takeda S, Aida M, Tasaka M, Kondo M, Nishimura M, Hara-Nishimura I (2008) NAC family proteins NARS1/NAC2 and NARS2/NAM in the outer integument regulate embryogenesis in *Arabidopsis*. *Plant Cell* 20: 2631–2642

Liang S-J, Wu H, Lun X, Lu D-W (2006) Secretory cavity development and its relationship with the accumulation of essential oil in fruits of *Citrus medica* L. var. *sarcodactlyis* (Noot.) Swingle. *J Integr Plant Biol* 48: 573–583

Lücker J, El Tamer MK, Schwab W, Verstappen FWA, Van Der Plas LHW, Bouwmeester HJ, Verhoeven HA (2002) Monoterpene biosynthesis in lemon (*Citrus limon*) cDNA isolation and functional analysis of four monoterpene synthases. *Eur J Biochem* 269: 3160–3171

Mandel MA, Feldmann KA, Herrera-Estrella L, Rocha-Sosa M, León P (1996) *CLA1*, a novel gene required for chloroplast development, is highly conserved in evolution. *Plant J* 9: 649–658

Martin DM, Aubourg S, Schouwey MB, Daviet L, Schalk M, Toub O, Lund ST, Bohlmann J (2010) Functional annotation, genome organization and phylogeny of the grapevine (*Vitis vinifera*) terpene synthase gene family based on genome assembly, FLcDNA cloning, and enzyme assays. *BMC Plant Biol* 10: 226–247

Muñoz-Bertomeu J, Arrillaga I, Ros R, Segura J (2006) Up-regulation of 1-Deoxy-D-xylulose-5-phosphate synthase enhances production of essential oils in transgenic spike lavender. *Plant Physiol* 142: 890–900

Ômura H, Honda K, Feeny P (2006) From terpenoids to aliphatic acids: Further evidence for late-instar switch in osmeterial defense as a characteristic trait of swallowtail butterflies in the tribe papilionini. *J Chem Ecol* 32: 1999–2012

Picaud S, Olsson ME, Brodelius M, Brodelius PE (2006) Cloning, expression, purification and characterization of recombinant (+)-germacrene D synthase from *Zingiber officinale*. *Arch Biochem Biophys* 452: 17–28

Rajaonarivony JIM, Gershenzon J, Croteau R (1992) Characterization and mechanism of (4*S*)-limonene synthase, A monoterpene cyclase from the glandular trichomes of peppermint (*Mentha*×*piperita*). *Arch Biochem Biophys* 296: 49–57

Sekiwa-Iijima Y, Moroi C, Hagiwara O, Kubota K (2002) Comparative analysis of volatile compounds from Japanese pepper (*Zanthoxylum piperitum* DC, Japanese pepper) by dynamic head space gas analysis. *Nippon Shokuhin Kagaku Kogaku Kaishi* 49: 320–326 (in Japanese)

Srividya N, Davis EM, Croteau RB, Lange BM (2015) Functional analysis of (4*S*)-limonene synthase mutants reveals determinants of catalytic outcome in a model monoterpene synthase. *Proc Natl Acad Sci USA* 112: 3332–3337

Starks CM, Back K, Chappell J, Noel JP (1997) Structural basis for cyclic terpene biosynthesis by tobacco 5-epi-aristolochene synthase. *Science* 277: 1815–1820

Takada S, Hibara K-I, Ishida T, Tasaka M (2001) The CUP-SHAPED COTYLEDON1 gene of Arabidopsis regulates shoot apical meristem formation. *Development* 128: 1127–1135

Talavera G, Castresana J (2007) Improvement of phylogenies after removing divergent and ambiguously aligned blocks from protein sequence alignments. *Syst Biol* 56: 564–577

Tamura K, Stecher G, Peterson D, Filipski A, Kumar S (2013) MEGA6: molecular evolutionary genetics analysis version 6.0. *Mol Biol Evol* 30: 2725–2729

Tanaka M, Esaki T, Kenmoku H, Koeduka T, Kiyoyama Y, Masujima T, Asakawa Y, Matsui K (2016) Direct evidence of specific localization of sesquiterpenes and marchantin A in oil body cells of *Marchantia polymorpha* L. *Phytochemistry* 130: 77–84

Uji Y, Ozawa R, Shishido H, Taniguchi S, Takabayashi J, Akimitsu K, Gomi K (2015) Isolation of a *sesquiterpene synthase* expressing in specialized epithelial cells surrounding the secretory cavities in rough lemon (*Citrus jambhiri*). *J Plant Physiol* 180: 67–71

Voirin B, Bayet C (1996) Developmental changes in the monoterpene composition of *Mentha*×*piperita* leaves from individual peltate trichomes. *Phytochemistry* 43: 573–580

Voo SS, Grimes HD, Lange MB (2012) Assessing the biosynthetic capabilities of secretory glands in *citrus* peel. *Plant Physiol* 159: 81–94

Yamasaki Y, Akimitsu K (2007) *In situ* localization of gene transcriptions for monoterpene synthesis in irregular parenchymic cells surrounding the secretory cavities in rough lemon (*Citrus jambhiri*). *J Plant Physiol* 164: 1436–1448

Zhou Y-F, Mao S-L, Li S-F, Ni X-L, Li B, Liu W-Z (2014) Programmed cell death: A mechanism for the lysigenous formation of secretory cavities in leaves of *Dictamnus dasycarpus*. *Plant Sci* 225: 147–160

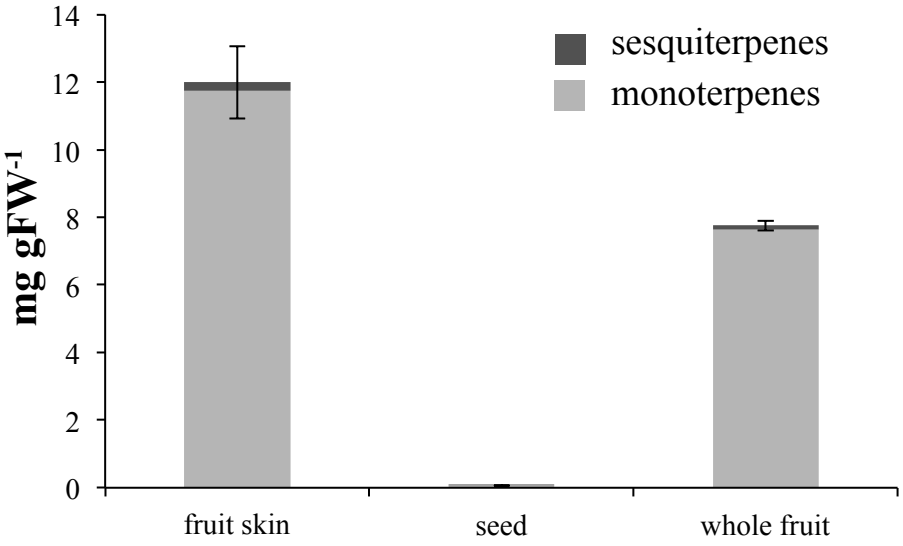

Supplementary Figure S1. Terpene amount in fruit skin, seeds, and whole fruits of Japanese pepper. Monoterpenes (β-phellandrene, D-limonene, and citronellal) and sesquiterpenes (β-caryophyllene and germacrene D) are indicated by gray and black, respectively. Mean values ± SE are shown (*n*=3).

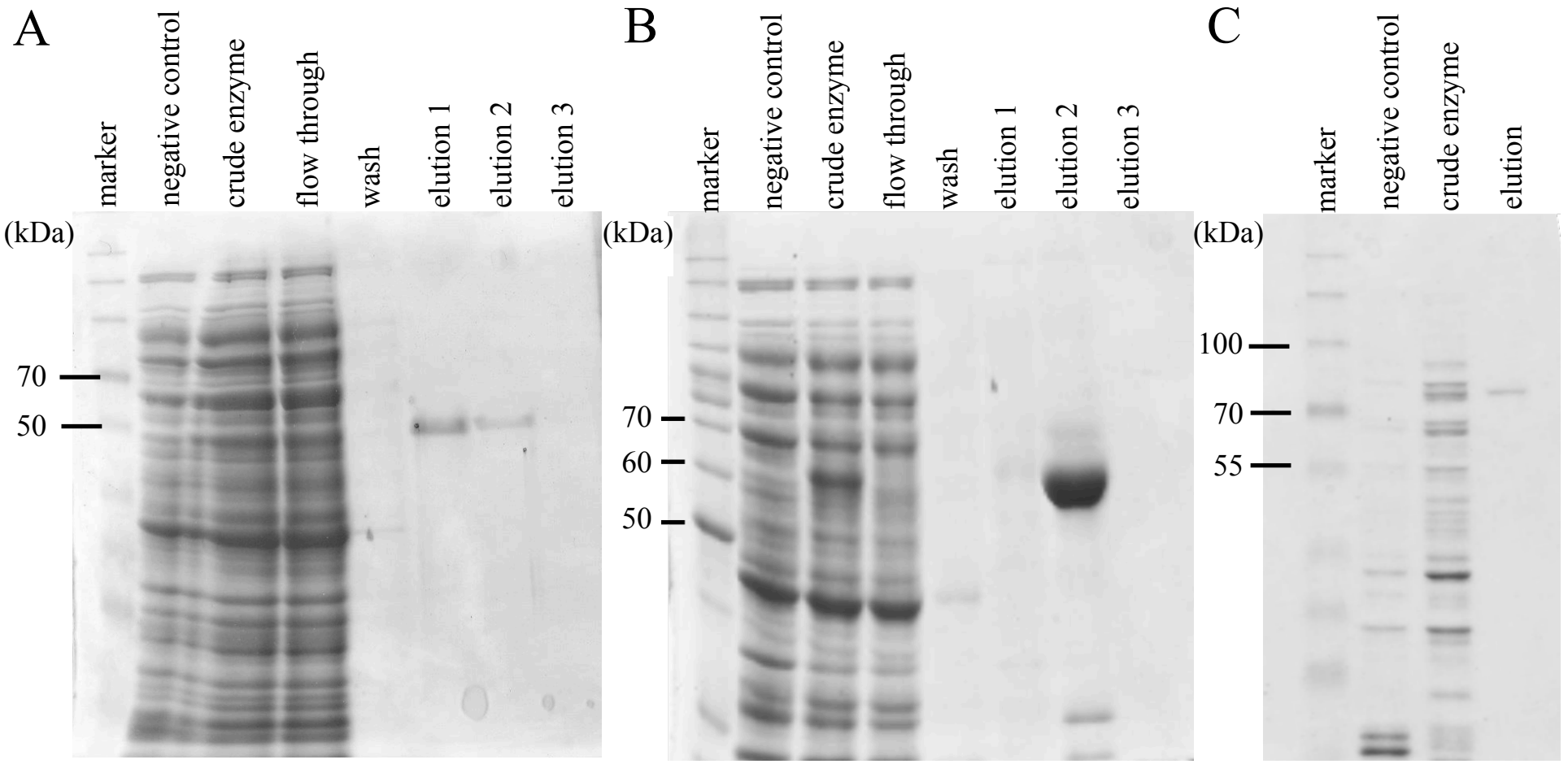

Supplementary Figure S2. SDS-PAGE analysis of ZpTPSs. ZpTPS1 (A) and ZpTPS2 (B) were produced as His-tagged proteins and purified using Ni^{2+} affinity chromatography. ZpTPS3 (C) was produced as a GST-fusion protein and purified using Glutathione Sepharose 4B.

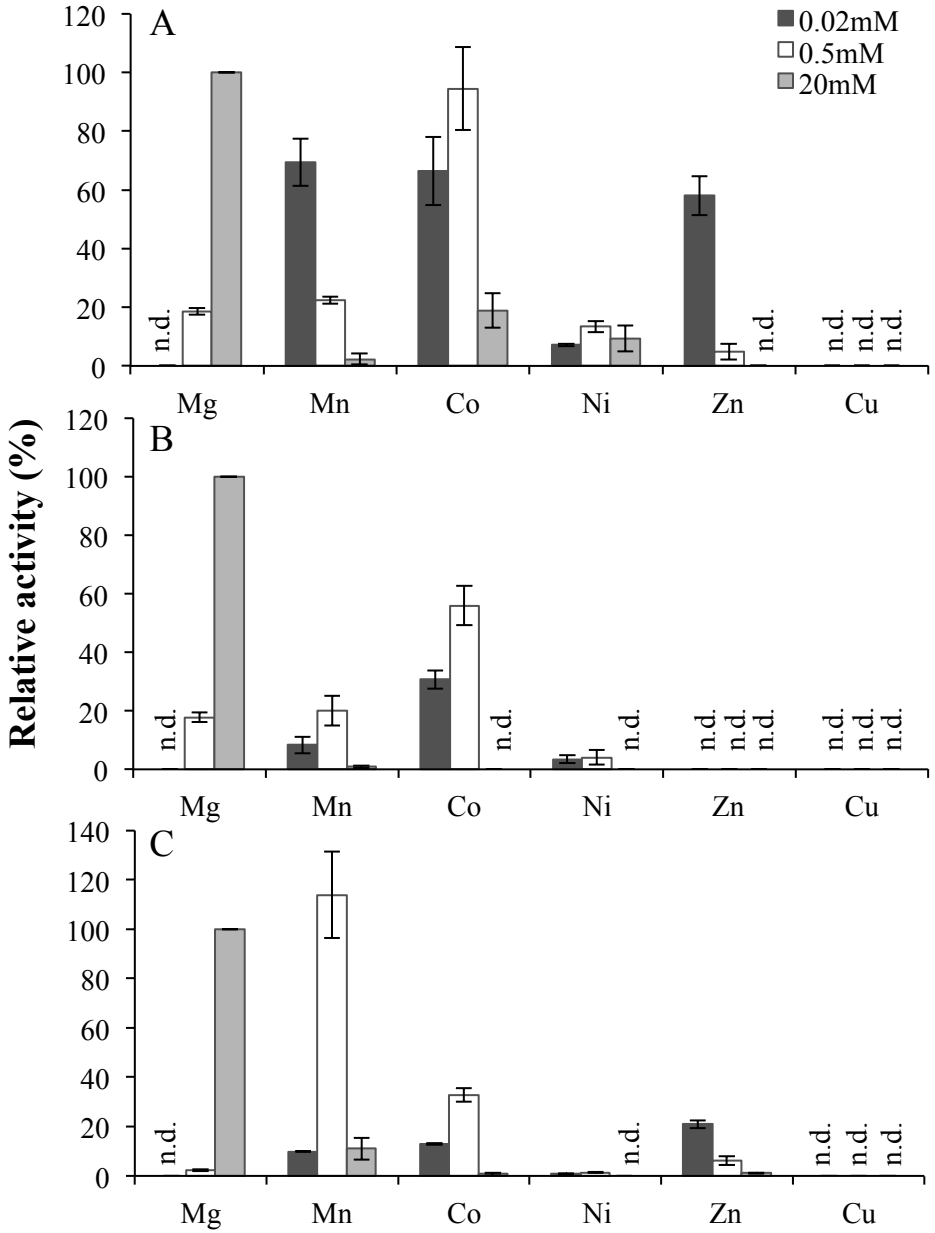

Supplementary Figure S3. Effects of divalent metal ions of varying concentration on the enzymatic activity of ZpTPSs. (A) ZpTPS1, (B) ZpTPS2, and (C) ZpTPS3 activity in the presence of different divalent cations. Mean values ± SE are shown (*n*=3).

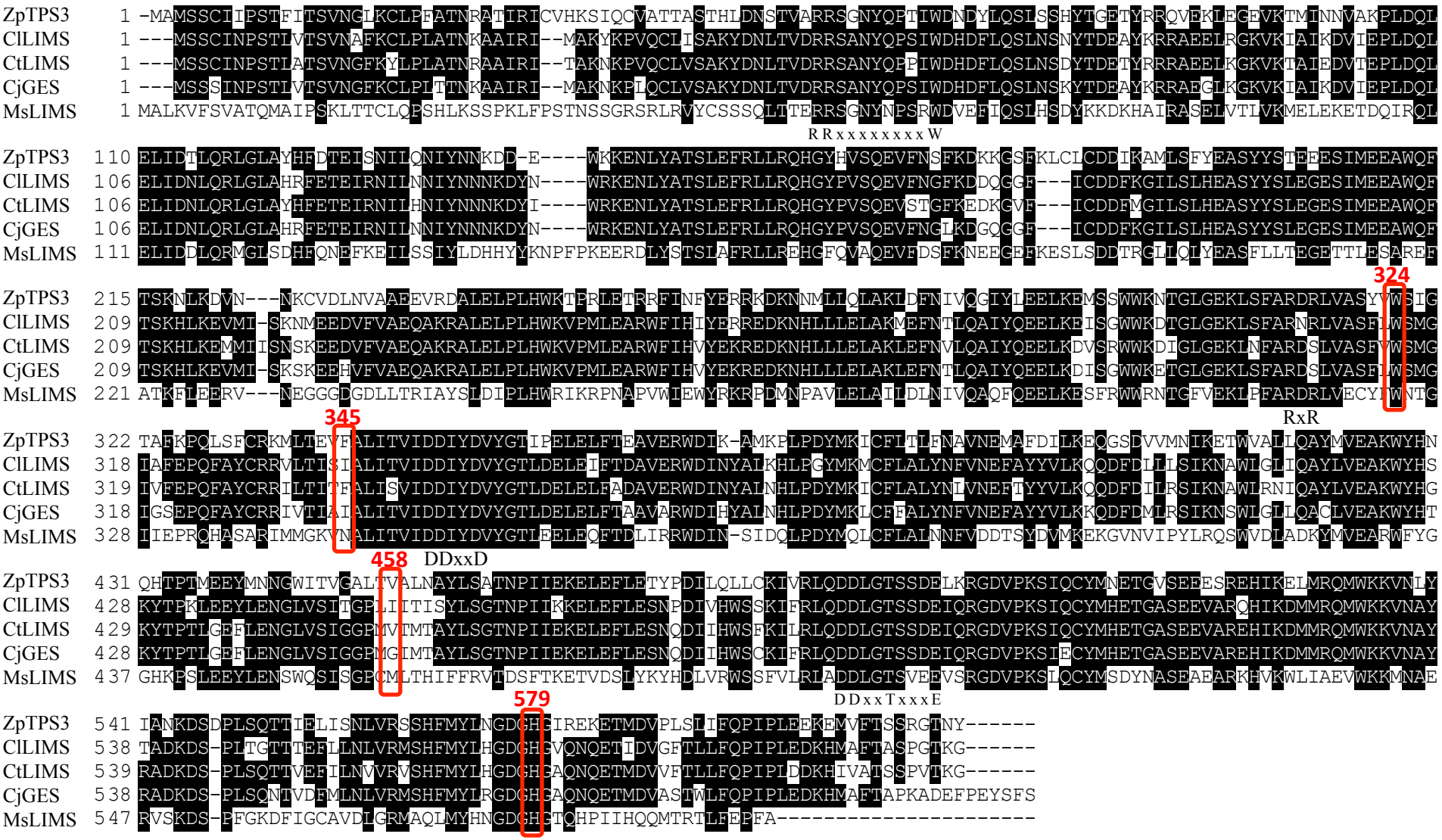

Supplementary Figure S4. Amino acid sequence alignment of ZpTPS3, limonene synthase from *Citrus limon* (ClLIMS; AAM53944.1), *Citrus trifoliate* (CtLIMS; BAG74774.1) and *Mentha spicata* (MsLIMS; AGN90912.1), and geraniol synthase from *Citrus jambhiri* (CjGES; BAM29049.1). The program GENETYX-MAC Ver.12.2.0 was used for the alignment. Black highlighting indicates those residues with more than 50% conservation among all sequences. The canonical highly conserved regions are labeled with RR(x)8W, RxR, DDxxD and DDxx(S,T)xxxE (Huang et al. 2013). The important residues (W324, N345, M458 and H579) for catalytic activity of MsLIMS (Srividya et al. 2015) are indicated by red squares.

Supplementary Table S1. Accession numbers of protein sequences used for phylogenetic analysis of plant TPSs.

Protein name	Accession number
Antirrhinum majus myrcene synthase	AAO41727.1
Antirrhinum majus β-ocimene synthase	AAO42614.1
Arabidopsis lyrata linalool synthase	XP_002886523.1
Arabidopsis thaliana β-caryophyllene synthase	AAO85539
Arabidopsis thaliana cdp synthase	Q38802.1
Arabidopsis thaliana kaurene synthase	AAC39443.1
Cannabis sativa α-pinene synthase	ABI21838
Citrus hystrix germacrene D synthase	ADX01384
Cirtus jambhiri δ-elemene synthase	BAP74389
Citrus jambhiri geraniol synthase	BAM29049.1
Citrus limon limonene synthase	AAM53944.1
Citrus trifoliate limonene synthase	BAG74774.1
Citrus unshiu β-ocimene synthase	BAD91046.1
Citrus unshiu β-pinene synthase	BAD27260
Clarkia breweri linalool synthase	AAD19840.1
Clarkia concinna linalool synthase	AAD19839.1
Cucurbita maxima kaurene synthase	AAB39482.1
Glycine soja linalool synthase	KHN36571.1
Gossypium arboreum δ-cadinene synthase	CAA76223.1
Gossypium arboreum myrcene synthase	KHG20211.1
Lavandula angustifolia β-phellandrene synthase	ADQ73631.1
Matricaria recutita β-caryophyllene synthase	AFM43734
Mentha aquatica linalool synthase	AAL99381.1
Mentha spicata limonene synthase	AGN90912.1
Mikania micrantha β-caryophyllene synthase	ACN67535
Morus notabilis myrcene synthase	EXB31237.1
Ocimum basilicum geraniol synthase	AAR11765.1
Ocimum basilicum germacrene D synthase	AAV63786
Oryza sativa Japonica Group β-caryophyllene synthase	ABJ16553
Oryza sativa Japonica Group farnesol synthase	ABJ16554
Phyla dulcis β-caryophyllene synthase	AFR23370
Picea sitchensis limonene synthase	ABA86248.1
Pinus taeda α-farnesene synthase	AAO61226.1
Pinus taeda α-pinene synthase	AAO61228.1
Pogostemon cablin germacrene D synthase	AAS86322
Populus trichocarpa cdp synthase	EEE93773.1
Populus trichocarpa kaurene synthase	XP_002311286.1
Solanum lycopersicum β-caryophyllene synthase	ADD96698
Solanum lycopersicum cineole synthase	AEM05857.1
Solanum lycopersicum linalool synthase	AEM05855.1
Thymus caespititius α-terpineol synthase	AGK88257.1
Vitis vinifera β-caryophyllene synthase	ADR74221
Vitis vinifera geraniol synthase	NP_001267920.1
Vitis vinifera germacrene D synthase	AAS66357.1
Vitis vinifera α-pinene synthase	ADR74203.1
Zea mays cdp synthase	AAT70084.1
Zingiber officinale germacrene D synthase	AAX40665
Zingiber zerumbet α-humulene synthase	BAG12315.1

Supplementary Table S2. RPKM of biosynthetic genes for volatile terpene formation.

Feature ID	Gene length	Green fruit	Ripe fruit
sesquiterpene synthase-like gene			
Zanthoxylum21_contig00027846 (ZpTPS1)	1793	13.7	0.8
Zanthoxylum21_contig00006748 (ZpTPS2)	1915	112.2	1.0
Zanthoxylum21_contig00011403	731	21.4	30.0
Zanthoxylum21_contig00011404	349	14.4	1.4
Zanthoxylum21_contig00014497	670	15.0	6.7
monoterpene synthase-like gene			
Zanthoxylum21_contig00008921 (ZpTPS3)	2293	10.2	3.7
Zanthoxylum21_contig00000439	2284	41.8	45.3
Zanthoxylum21_contig00007231	644	19.1	12.4
Zanthoxylum21_contig00008263	1906	15.8	13.1
Zanthoxylum21_contig00009768	642	27.0	36.4
Zanthoxylum21_contig00020015	227	4.9	4.4
geranyl diphosphate synthase-like gene			
Zanthoxylum21_contig00010188	1726	23.0	42.1
Zanthoxylum21_contig00011418	1133	17.7	17.6
farnesyl diphosphate synthase-like gene			
Zanthoxylum21_contig00008866	1401	29.9	16.3
Zanthoxylum21_contig00010526	1424	6.7	3.5
Zanthoxylum21_contig00013264	482	20.8	32.0